Scientific Research Publishing

Advances in Microbiology, 2020, 10, 166-179
https://www.scirp.org/journal/aim
ISSN Online: 2165-3410
ISSN Print: 2165-3402

ZnO/CdS Nanocomposite: An Anti-Microbial and Anti-Biofilm Agent

Haribhau Gholap[1*], Akash Gholap[2], Rajendra Patil[3*]

[1]Department of Physics, Fergusson College, Pune, India
[2]College of Pharmacy, Mula Education Society Sonai, Ahmednagar, India
[3]Department of Biotechnology, Savitribai Phule Pune University, Pune, India
Email: *harishgholap@gmail.com, agholap092@gmail.com, *rpatil@unipune.ac.in

How to cite this paper: Gholap, H., Gholap, A. and Patil, R. (2020) ZnO/CdS Nanocomposite: An Anti-Microbial and Anti-Biofilm Agent. *Advances in Microbiology*, **10**, 166-179.
https://doi.org/10.4236/aim.2020.104013

Received: December 24, 2019
Accepted: April 18, 2020
Published: April 21, 2020

Abstract

Microbial infectious are becoming a global threat, which is a reason for rise in mortality of human beings. One of the reasons for this mortality has been the drug resistance in microbes. The drug resistance poses a major challenge for effective control of microbial infections, and this threat has prompted us to search for alternative strategy to control the microbial infections. Recently, nanomaterials have emerged as an alternative to conventional platforms because they combine multiple mechanisms of action into one platform due to the distinctive properties of nanosized materials. In the present research we have attempted to synthesize ZnO/CdS nanocomposite for its application as an antimicrobial agent. We have characterized the synthesized nanocomposites by X-ray diffraction (XRD), ultraviolet-visible spectroscopy (UV-Vis), photoluminescence spectroscopy (PL), field emission scanning electron microscopy (FESEM) and high-resolution transmission electron microscopy (HRTEM). The nanocomposites have exhibited good antibacterial property against Gram positive and Gram-negative organisms by virtue of the generation of reactive oxygen species (ROS) inside the cells, as reflected by ruptured appearances in the FESEM micrographs. Apart from antimicrobial activity, it also inhibited biofilm formations in *Pseudomonas aeruginosa*, a causative organism in lung infection and burn associated infections.

Keywords

ZnO/CdS, Antimicrobial, Biofilm, *Pseudomonas*, *Bacillus*, *Escherichia*

1. Introduction

Emergence of the antibiotics resistance in pathogens has become a serious health problem which requires an immediate attention. It is known that over 70% of

bacterial infections are resistant to one or more of the antibiotics that are generally used to eradicate the infection [1]. There are in general two reasons for antimicrobial resistance; one being the misuse or overuse of antibiotics and second being the ability of microorganisms to form biofilm, a more prominent issue [2]. Biofilms are defined as conglomerations of bacterial cells and it remains with extra polymeric substance (EPS). EPS behaves as diffusion barrier and does not allow an entry of antibiotics inside the biofilm, thereby protecting cells residing inside the biofilm. The consequences of the restricted entry of antibiotics inside biofilm allow cells to grow and proliferate by drawing nutrients from biofilm, eventually emerging as multidrug resistant pathogens [3]. In the medical science, a recent survey shows that up to 60% of all human infections are owing to the biofilm. Therefore, effective strategies which will eradicate the microorganisms and biofilm have become a need of an hour [4]. In this regard, nanomaterials owing to their nanosized effect (higher surface to volume ratio) showed unique physical and chemical properties different from bulk materials which offer wide applications in various fields. Recently, metal nanoparticles have been reported for antimicrobial and antibiofilm activities [5]. However, semiconductor metal oxide nanostructures are better over all existing nanocomposites owing to very good property of photon absorption as well as efficient transport of photogenerated electron hole charge carriers [6]. Among semiconductor metal oxide, e.g. zinc oxide (ZnO) is tremendously explored due to wide band gap energy of 3.37 eV and large exciton binding energy (60 meV) [7]. Another reason for wide applications of ZnO nanoparticles in antimicrobial and antimicrobial research has been its constant photo-catalytical activities under harsh processing conditions [8]. Upon illumination, ZnO nanoparticles generate the electron hole pairs, and produce reactive oxygen species (ROS), which oxidizes organic matter and, thus, imparts biocidal property to ZnO [9]. However, ZnO nanoparticles are having a very low efficiency for the separation of electron hole pairs due to fast recombination of charge carriers [10]; therefore, efforts have been made to suppression of the recombination of photogenerated electron-hole pairs in ZnO nanoparticles. In this regard, ZnO nanoparticles have been doped or conjugated with other nanoparticles such as ZnO/CdTe for antimicrobial applications [11], ZnO/CdSe for photoelectrode for splitting water [12], ZnO/CdS for enhanced field emission behavior [13], ZnO/CdS for enhanced photocatalytic activity [14], ZnO/CdS for antibacterial activity [15], ZnO/CdS for enhanced photocatalytic H_2 evolution [16], and ZnO/CdS nanocomposite for Solar cell [17]. Herein, we have attempted to enhance the photocatalytic efficiency ZnO nanoparticles by synthesizing a composite with CdS nanoparticles, and further evaluated its antimicrobial and antibiofilm.

2. Materials and Methods

2.1. Chemicals

The as-synthesized ZnO/CdS nanocomposites were synthesized by using analyt-

ical grade zinc nitrate hexahydrate ($Zn(NO_3)_2{\cdot}6H_2O$, 98%), potassium hydroxide (KOH, 99%), cadmium nitrate ($Cd(NO_3)_2$), thiourea ($SC(NH_2)_2$), polyvinyl pyrrolidone (PVP), without further purifications.

2.2. Synthesis of ZnO Nanostructure

In the typical of ZnO nanostructures, 1 mmol of Zn $(NO_3)_2{\cdot}6H_2O$ and 5 mmol of KOH were dissolved in 100 mL aqueous solution. Then mixture immediately transferred into a Teflon-lined stainless-steel autoclave. The hydrothermal synthesis was carried out at 120˚C etc. for 2 h duration. After completion of the synthesis duration, product washed with distilled water and dried in oven at 70˚C.

2.3. Synthesis of ZnO-CdS Heterostructures

In addition to ZnO synthesis process 0.63 mM $Cd(NO_3)_2$, 1.9 mM PVP and 0.0150 g $SC(NH_2)_2$ were added. Then mixture immediately transferred into a Teflon-lined stainless-steel autoclave (200 mL). The hydrothermal synthesis was carried out at temperatures 120˚C etc. for 2 h duration. After completion of the synthesis duration, product washed with distilled water and dried in oven at 70˚C.

2.4. Antimicrobial Study

Antimicrobial study was performed by measuring growth inhibition ability of ZnO nanostructures and ZnO/CdS nanocomposite by using model organisms such as *Bacillus subtilis* NCIM 2063 and *Escherichia coli* NCIM 2931 via colony count method under 60 - 100 Lux intensity of visible light. ZnO nanostructures and ZnO/CdS nanocomposite in the concentration range of 0 to 20 μg/mL each were added to Muller Hinton broth, and each one separately inoculated with *B. subtilis* and *E. coli* (final cell density of 1×10^6 colony forming units per mililitre (CFU/mL)) and incubated at 37˚C for 15 h. After 15 h, viable numbers of cells were recorded as CFU/mL in comparison to control (without nanomaterials). The data were confirmed as survival rates (CFU/mL), (100% survival in control). Morphological alterations on the surface of microorganisms were observed under FESEM. In short, the cells of *B. subtilils* and *E. coli* were grown to mid log phase (approximately 1×10^7 cells/mL) and treated with respective MIC concentration of ZnO and ZnO/CdS nanocomposite for 3 h at 37˚C and 200 r.p.m. The cells were collected by centrifugation at 11,000 g for 15 min at 4˚C. The pellets were then washed 3 times with 0.1 M phosphate buffer of pH 7.4 and fixed in 2.5% glutaraldehyde at 4˚C for 4 h. After rinsing 2 - 3 times with buffer, the pellets were dehydrated in ethanol serials (10% - 100%, 20 min per step), and then dried in air. Finally, the images were seen under FESEM [18].

2.5. Antibiofilm Study

Antibiofilm study of ZnO and ZnO/CdS nanocomposite was studied in Pseu-

domonas aeruginosa at 60 - 100 Lux intensity of visible light. It was carried out by using crystal violet retention assay because crystal violet has an affinity towards polysaccharides of biofilm. In summary, the *P. aeruginosa* was grown overnight in Luria Bertaini (LB) medium at 37˚C with agitation. Later, the culture was diluted with LB medium (OD600—0.02), and 50 µL of the diluted culture was added to 950 µL of LB medium and allowed to form biofilm. After formation of biofilm on polystyrene plastic surfaces, the planktonic cells (cells which are suspended in the medium) were replaced with fresh medium supplemented with 0 - 125 µg/mL ZnO and ZnO/CdS nanocomposite, separately, and incubated statically for 20 h at 37˚C. After incubation, planktonic bacteria were removed, and the biofilms were washed 2 - 3 times with phosphate buffered saline buffer. Washed biofilms were fixed with 1 mL of methanol. After 15 min, the methanol was removed, and the plates were dried at room temperature. Crystal violet (0.1% in water) was then added to each well (1 mL/well), and the plates were incubated for 15 min at room temperature. Crystal violet was then removed, and stained biofilms were washed three times with 1 mL of water. Acetic acid (33% in water) was added to the stained biofilms in order to solubilize the crystal violet, and the absorbance of the solution was read at 590 nm with a spectroscopy (Schimadzu, Japan) [18].

3. Result & Discussion

3.1. X-Ray Diffraction (XRD)

A typical XRD patterns of ZnO (red coloured) & ZnO/CdS (black colored) nanocomposites (**Figure 1(a)** and **Figure 1(b)**), show a set of well-defined crystal planes are indexed to the hexagonal wurtzite phase, with lattice constants, a = 0.325 nm and b = 0.520 nm (JCPDS: 36-1451) & ZnO/CdS nanocomposite exhibits a set of well-defined crystal planes are indexed to the hexagonal wurtzite phase of ZnO (a = 0.3249 nm and c = 0.5206 nm; JCPDS File: 036-1451) and observation of the diffraction spectrum shows the occurrence of some low intensity crystal planes, which are indexed to the cubic phase of CdS (JCPDS File: 080-0019). The crystal planes correspond to the (111), (220) and (311) of cubic CdS (shown in the inset). CdS nanoparticle has a higher full width half maxima (FWHM) of the crystal planes due to smaller nanoparticle size compare to ZnO. No crystal planes corresponding to other phases or impurities were observed. Thus, the XRD results evidently show the formation of ZnO/CdS nanocomposite.

3.2. Optical Properties

The optical properties of ZnO and ZnO/CdS nanocomposite samples were studies by UV-visible diffused reflectance (UV-Vis-DRS) and photoluminescence spectroscopy (PL) at taken at room temperature. The UV-visible diffused reflectance (UV-Vis-DRS) of ZnO/CdS nanocomposite was shown in **Figure 1(d)**. The spectrum of only ZnO nanostructure which illustrates the sharp absorption band

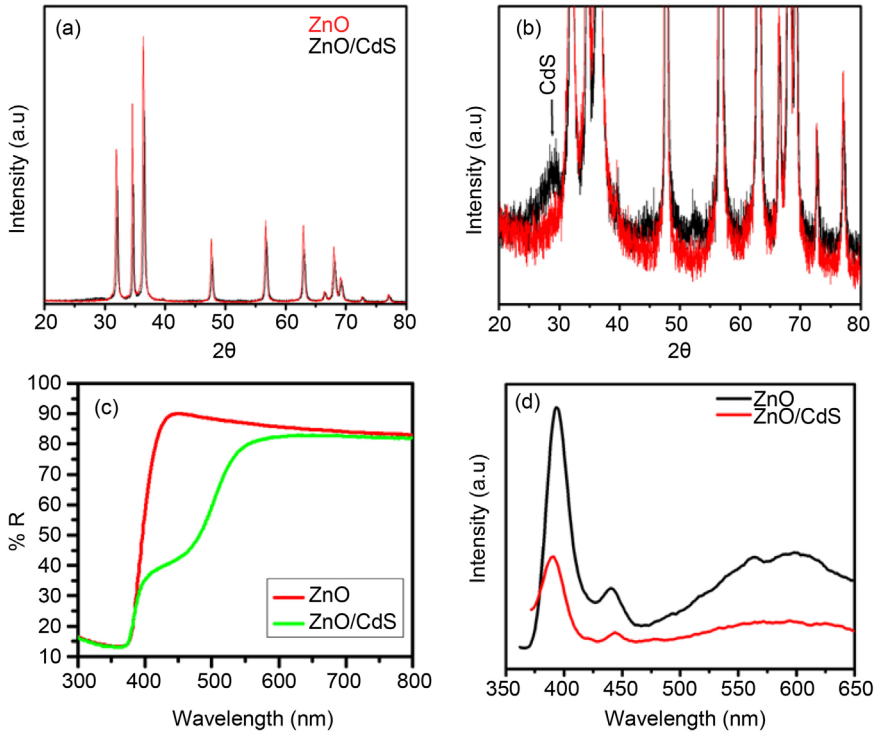

Figure 1. (a) XRD of ZnO and ZnO-CdS nanocomposite; (b) (Inset) XRD of ZnO and ZnO-CdS nanocomposite, (c) UV-Vis-DRS spectra of ZnO and ZnO-CdS nanocomposite; (d) PL spectra of ZnO and ZnO-CdS nanocomposites.

at 385 nm (3.22 eV) was known to originate from the band-edge absorption and with no apparent absorption in the visible region. In case of ZnO/CdS nanocomposite, the absorption spectra in which the band edges at ~385 (3.22 eV) and 520 nm (2.38 eV) are corresponds to the ZnO and CdS, respectively (**Figure 1(c)**). The two band edges feature in the typical spectra clearly shows the formations of nanocomposite between the UV region band (ZnO) and visible region (CdS).

3.3. Photoluminescence Spectroscopy (PL)

In order to shows the influence of CdS nanoparticles on the electronic properties of ZnO, the PL spectra of the ZnO in the range of 350 - 650 nm at room temperature is shown in **Figure 1(c)**. In the case of pure ZnO, a narrow UV band emission at 393 nm was observed, which can be assigned to exciton recombination, a strong blue emission at ~400 - 450 nm, and a broad green band at about 554 nm as well as a strong emission at 596 nm in the yellow region, which can be attributed to intrinsic defects in ZnO as oxygen interstitials dominates the PL spectrum [19]. The intensity of the characteristic peaks in the PL spectrum of ZnO/CdS nanocomposite was smaller than that for the ZnO. The observed decrease in the overall intensity of the PL spectrum is attributed to the decrease in the oxygen vacancies [20]. We also assume that flakes like structure on the surface would possess more defects due to the faster one-dimensional (1D) crystal

growth. The PL emission band shift in the visible region ~520 nm of spectrum and could be attributed to the interaction between the two semiconductors of ZnO and CdS. The change in the wavelength can be ascribed to the change in oxygen vacancy centers around CdS. The broad emission peak centered at ~520 nm (which corresponds to the green-yellow emission) can be ascribed to the shallow defect transition of CdS nanoparticles. The decrease in the hydroxyl species on the ZnO surface is due to the presence of the CdS nanoparticles in the nanocomposite [21] [22]. The conduction band edge of CdS is above to that of the ZnO. When the visible light incident on ZnO/CdS nanocomposite the excited electron-hole pairs are generated. Owing to the explicit nature of the band alignment at the interface of ZnO/CdS nanocomposite, the generated electrons are moving to the conduction band of ZnO, at the same time as the holes with the valence band of the CdS. These alienated electrons and holes have a drastically improved recombination lifetime of electron-hole pairs, and so available for redox reactions, and may play a vital role in the inhibition of growth/biofilm by the nanocomposite, as discussed further in the text.

3.4. Morphology

The morphology of ZnO nanoparticles was studies by FESEM (**Figures 2(a)-(c)**). It's well-defined flakes-like three-dimension (3D) microstructures with diameters in the range of 1 - 2 μm. A close-up view of the nanosheets-built flakes-like microstructures reveals that the nanosheets are about ~10 nm in thickness, and they alternately connect with each other to form a network-like surface of the "flakes." Similarly, in case ZnO/CdS heterostructures (**Figures 2(d)-(f)**), the CdS nanoparticles were seen on the surface of flake like ZnO with

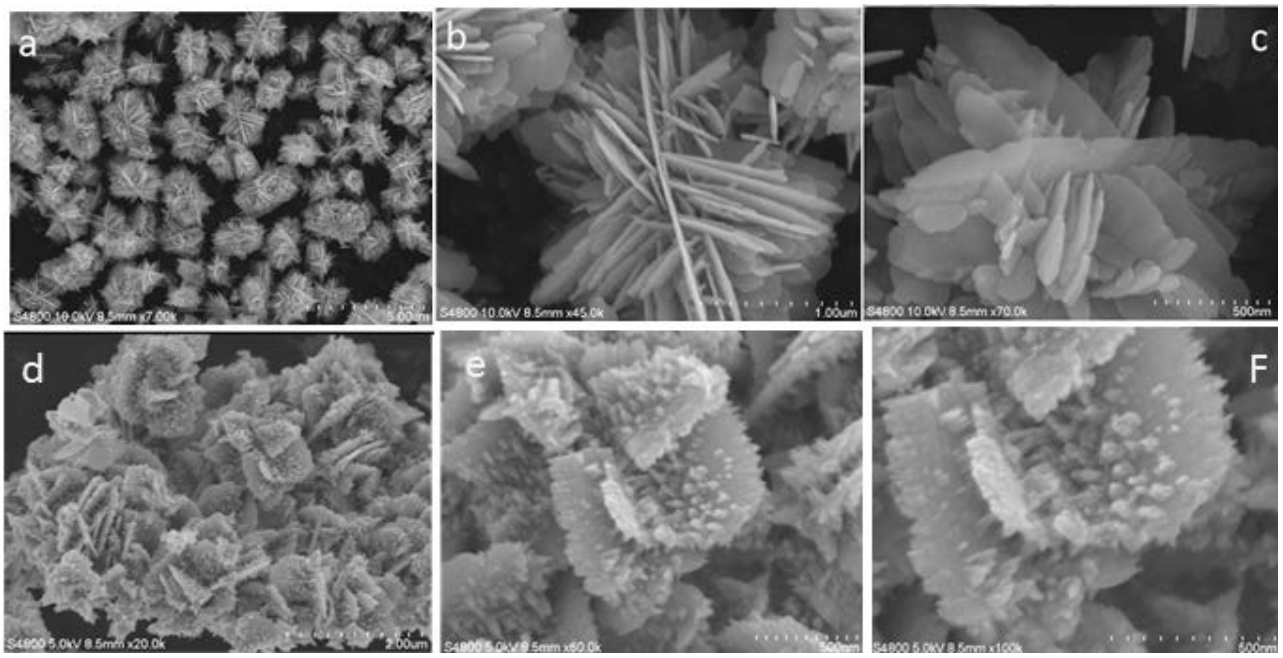

Figure 2. FESEM micrographs of ZnO ((a)-(c)) and ZnO/CdS nanocomposite ((d)-(f)).

average size ~15 - 20 nm. Further the morphological and structural analysis of ZnO and ZnO/CdS was carried out using TEM and HRTEM (Figure 2 and Figure 3). Flakes like ZnO microstructure were observed under TEM, confirming the hierarchical 3D structure with diameter around 1 - 2 μm, constructed by numerous nanosheets which have uniform thickness of ~10 nm (Figures 2(a)-(c)) and HRTEM image shows typical well defined lattice fringes width 0.26 nm which corresponding to the growth orientation along (002) plane (Figures 3(a)-(c)). Similarly, in case of ZnO/CdS nanocomposite, TEM images show that the of CdS nanoparticles on the flakes of ZnO (Figures 2(d)-(f)) (a magnified image). Magnified view shows a single crystalline nature of ZnO and CdS which is marked by with red color circles. The average size of CdS nanoparticles were about ~8 - 10 nm. The appearance of rings along with spots in the SAED pattern of the ZnO/CdS may be due to orientation disorder between the ZnO nanoflakes and the CdS nanoparticles (Figure 3(f)).

3.5. Antibacterial

The effect of different concentrations of ZnO and ZnO/CdS nanocomposites on the growth of *B. subtilis* and *E. coli* was shown in Figure 4. When the cells of the model organisms were subjected to increasing concentrations of ZnO and ZnO/CdS nanocomposite, the viability of cells decreased. The initial number of

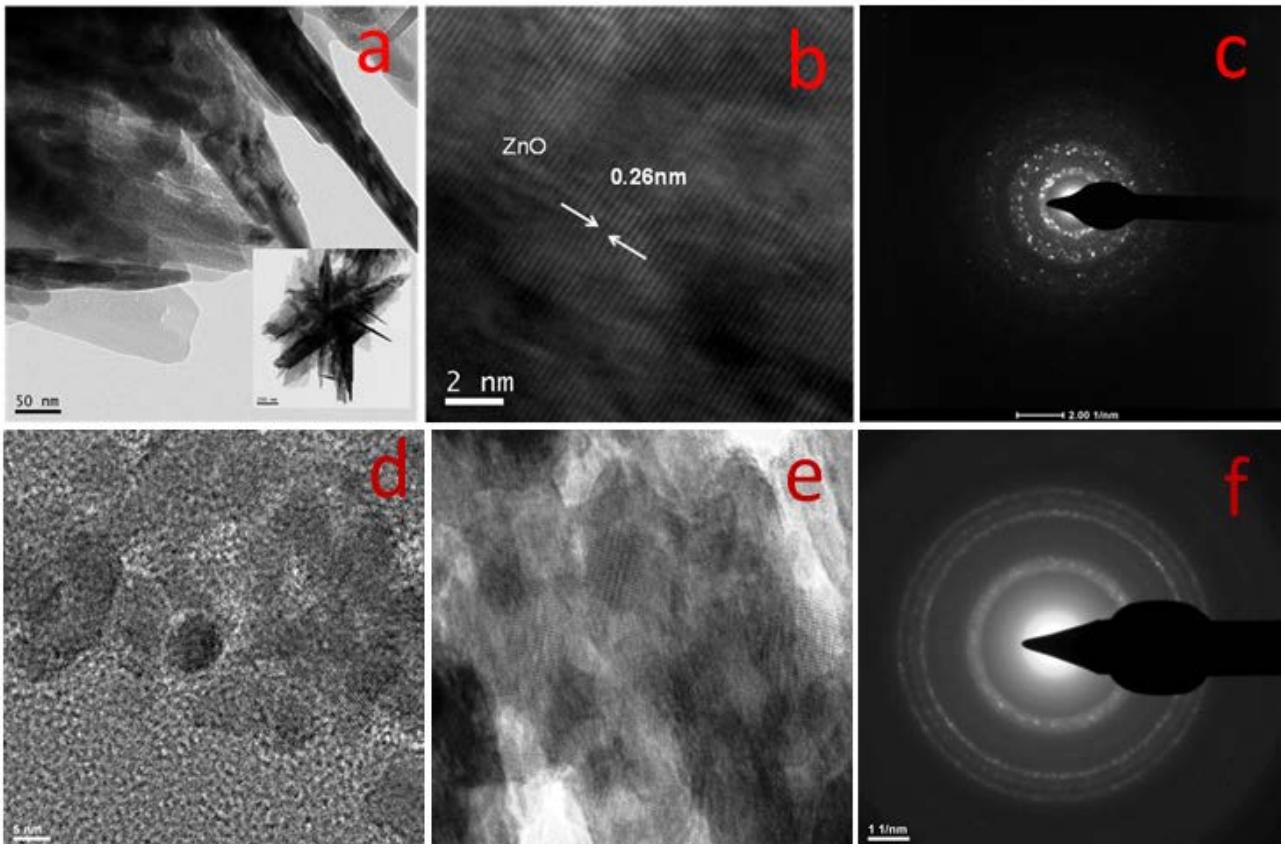

Figure 3. HRTEM micrographs of ZnO ((a) and (b)) and ZnO/CdS ((d)-(f)).

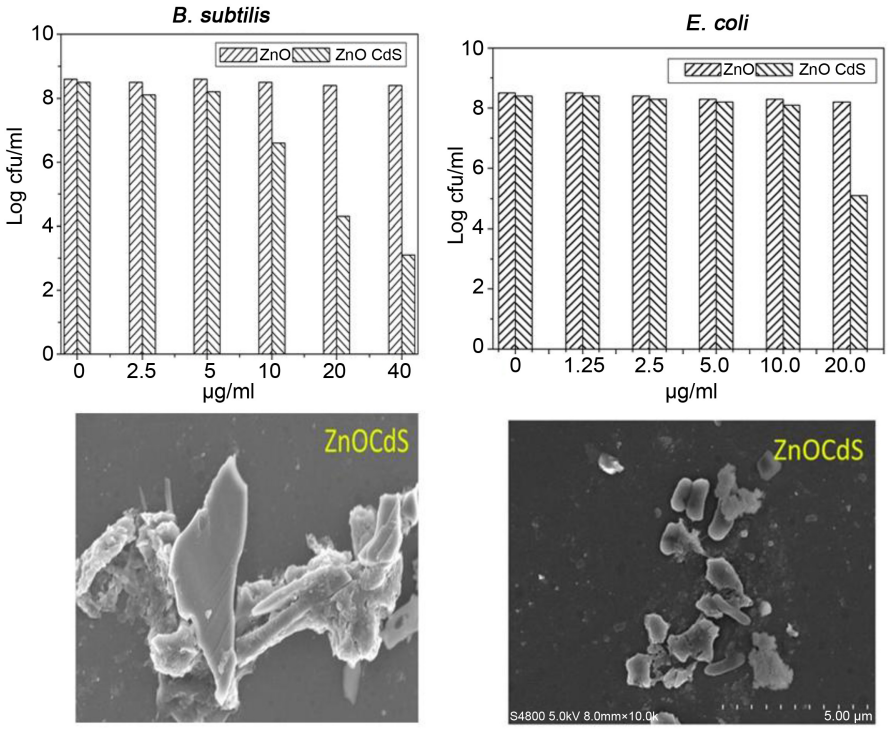

Figure 4. Antibacterial activities of ZnO and ZnO/CdS on *B. subtilis* and *E. coli* (upper panel) and SEM micrographs of *B. subtilis* (left) and *E. coli* (right) in presence of ZnO/CdS.

viable number bacterial cells, approximately 6 Log CFU/mL increased to approximately 9 Log CFU/mL at 0 µg/mL ZnO and ZnO/CdS nanocomposite after 18 hrs of incubation. This represents a 100% growth (**Figure 4**). Upon increasing concentration of ZnO and ZnO/CdS nanocomposites, it was observed that whereas ZnO had a little effect on the growth of microorganisms, ZnO/CdS has decreased the growth by 1 to 3 Log CFU/mL. The concentration of ZnO/CdS nanocomposites required to reduce 3 Log CFU/mL in *B. subtilis* and *E. coli* was 20 µg/mL. It is interesting to note that the ZnO/CdS nanocomposites have a dissimilatory action on *B. subtilis* and *E. coli*, it is more prominent on *B. subtilis*, due to difference in the cellular structures. *E. coli* possesses an extra outermost layer made up of lipopolysaccharides, therefore, acts as a permeable barrier and restricted the damages cause to the cytoplasmic membrane. Our findings agreed with previous reports [23] [24]. The other reason for the predominance action of ZnO/CdS nanocomposite on *E. coli* is due the polarity of cell membrane of *E. coli*. Microorganism *E. coli* has fewer negative charges than *B. subtilis*, and therefore allows greater penetration of free radical such as hydroxyl radicals (•OH), superoxide peroxide anions ($O_2^{\bullet-}$) in *B. subtilis* and a preferred action on *B. subtilis* [23].

Several suggestions have been proposed to explain the mechanism of antimicrobial action of ZnO nanocomposites. The release of Zn^{2+} has been suggested as one of the reasons for the antimicrobial activity [24]. According to this theory,

the toxicity of ZnO nanocomposite arose due to the dissolution of Zn^{2+} into the medium containing microorganisms. However, in our study, the Zn^{2+} leached into the medium were too less to inhibit the growth of microorganisms. Hence, we rule out this hypothesis. Oxidative stress mediated antimicrobial mechanisms of ZnO nanocomposites have also being suggested. According to this theory, the inactivation of bacteria by ZnO nanocomposites involves ZnO-mediated change in the permeability of membrane allowing the internalization of nanocomposites and induces the oxidative stress. However, when we assayed the molecular marker enzymes of oxidative stress viz., Catalase and Superoxide dismutase, we found that the expression levels of these two enzymes were like control. Secondly, the pore size in the cells wall of bacteria under study were small, approximately, 4 to 10 nm, so it was not practical possible to ZnO/CdS nanocomposite to enter the cell through cell membrane [25].

When the nanostructures interact with the cellular membrane of microorganisms in presence of sunlight, the electron and hole generated in which hole remains in the valence band and electron move towards the conduction band. Hence, while, electrons in the conduction band shows higher reducing power, where holes in the valence band shown higher oxidizing power [26]. As a result, when molecular oxygen reacts with electron, $O_2^{\bullet-}$ is produced in the conduction band through a reductive process. In the valence band, the hole abstracted electrons from the water and/or hydroxyl ions to generate $^{\bullet}OH$ through an oxidative process. Singlet oxygen (1O2) was mostly produced indirectly from aqueous reactions of $O_2^{\bullet-}$. Whereas $^{\bullet}OH$ is a strong and nonselective oxidant, it oxidizes the lipid bilayer of membrane and eventually ruptures the cell surfaces. The $^1O_2$ was the main mediator of phototoxicity and irreversibly damaged the treated cells, causing the cell membrane oxidation and degradation. Thus, the growth inhibition in *B. subtilis* and *E. coli* occurred owing to the direct action of the ZnO/CdS nanocomposites on the cell surfaces. When we observed the cellular morphology of *B. subtilis* and *E. coli* under FESEM, we observed the surface perturbation, in agreement with the previous reports [27]. The ZnO/CdS nanostructures act on microbial cells by generating ROS on cellular membrane, which virtually oxidizes every cellular component and ruptured the cell wall. Therefore, when observing cellular membrane by SEM, we observed irregular shaped cells with pits and ruptured appearances on surfaces (**Figure 4**). The surface perturbation in *B. subtilis* and *E. coli* agreed with the previous reports [28].

3.6. Anti-Biofilm

Biofilm is a severe problem in biomedical sector; the medical implants and indwelling devices are severely affected due to bacterial colonization and biofilm formation. The conventional antibiotic therapies have become ineffective against device-associated biofilm [29]. Thus, to overcome the inherent resistance of biofilms to antimicrobial agents, we explored ZnO/CdS nanocomposite on the biofilm of *P. aeruginosa*. The most distinguishing phenotype of the biofilm mode of

growth is its intrinsic resistance to antimicrobial treatment and immune response killing [30]. The cells of *P. aeruginosa* in presence of nutrient components of media tend to grow and form biofilm after 36 - 40 h. We assayed the biofilm by measuring the amount of crystal violet retained by biofilm, because crystal violet has an affinity towards the biofilm. Biofilm retains 100% crystal violet at 0 g/mL, however, biofilm retention was reduced to less than 35% at 50 μg/mL of ZnO/CdS nanocomposites. The formation of biofilm decreased with increase in the concentrations of ZnO/CdS nanocomposite. The disruption of biofilm is liable to extend the antimicrobial action of ZnO/CdS nanocomposite to the cells protected inside biofilm. Therefore, in order to know the viability of these cells inside biofilm, viable count of cells inside biofilm was performed. As can be seen from **Figure 5**, the cell viability inside biofilm after exposure

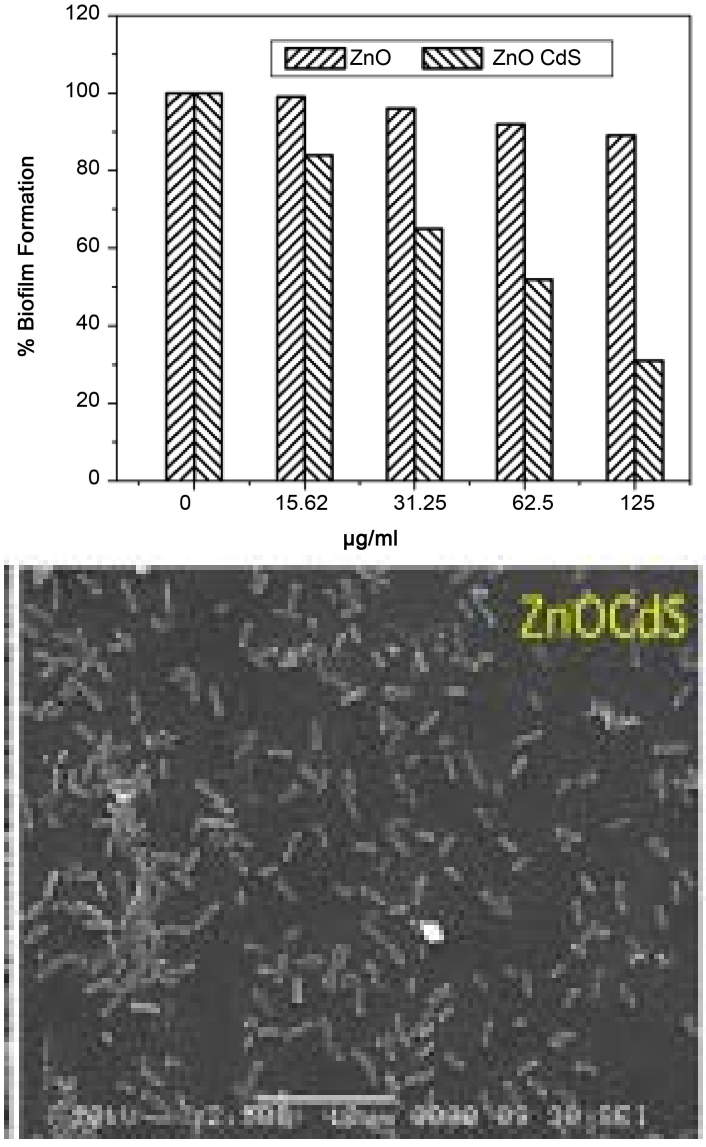

Figure 5. Antibiofilm activity of ZnO and ZnO/CdS on *P. aeruginosa* (upper panel). SEM of biofilm of *P. aeruginosa.*

ZnO/CdS nanocomposite decreased. At 0 g/mL, cells viability was 100%, however, viability decreased to 40% at 125 μg/mL of ZnO/CdS nanocomposites. The antibiofilm activity in *P. aeruginosa* was also supported by topographical observation of biofilm under FESEM at 50 μg/mL ZnO/CdS nanocomposite (**Figure 5**). Under FESEM, the biofilm of *P. aeruginosa*has been reported as a smooth layer of matrix with an under-covered uniform cell *i.e.* cells embedded in the polysaccharide's matrix [18], a typical of biofilm structure. However, at 50 μg/mL ZnO/CdS nanocomposite, a truncated biofilm was observed, with cells exposed to outer surfaces (**Figure 5**). The antibiofilm study is significant because the cells in the biofilm are not viable, and therefore, will not form biofilm. Earlier reports co-relate antibiofilm activity of nanomaterials due to anti-quorum sensing (anti-QS) sensing activity [31] [32]. In present study we rule out the QS mediated antibiofilm activity because our nanostructures also have brought about a reduction in the number of viable cells. We do not rule out the ROS mediated antibiofilm activity in *P. aeruginosa* because ROS species have been reported to carry out the oxidation of polysaccharides, proteins, and lipids biomolecules.

4. Conclusion

ZnO/CdS nanocomposites are promising applicant for the photocatalytic demolition of bacterial cells. ZnO/CdS nanocomposites are effective alternative to organic based drugs. Structural, optical and morphological data confirm the successful synthesis of ZnO/CdS nanocomposite. ZnO/CdS nanocomposites have shown antimicrobial activity against *B. subtilis* and *E. coli*, and the enhancement in antibacterial property by ZnO/CdS nanocomposite was concentration dependent. The ruptured appearances on bacterial cell surfaces indicate cellular membrane damage by ZnO/CdS nanocomposites. The decline in the development of biofilm in *P. aeruginosa* in the presence of ZnO/CdS nanocomposite shows that it is one of the excellent materials for inhibiting biofilm formations in other clinically pathogenic biofilm forming organisms. ZnO/CdS nanocomposites not only showed antibiofilm activity in *P. aeruginosa*, but it also inhibited the microbial population inside the biofilm and eliminates the biofilm forming ability of the microorganisms.

Acknowledgements

Rajendra Patil acknowledges support from Department Research Grants of Savitribai Phule Pune University, Pune University.

Conflicts of Interest

The authors declare no conflicts of interest regarding the publication of this paper.

References

[1] Aslam, B., Wang, W., Arshad, M.I., Khurshid, M., Muzammil, S., Rasool, M.H., Ni-

sar, M.A., Alvi, R.F., Aslam, M.A., Qamar, M.U., Salamat, M.K.F. and Baloch, Z. (2018) Antibiotic Resistance: A Rundown of a Global Crisis, Infection and Drug Resistance. *Infection and Drug Resistance*, **11**, 1645-1658. https://doi.org/10.2147/IDR.S173867

[2] Li, B. and Webster, T.J. (2018) Bacteria Antibiotic Resistance: New Challenges and Opportunities for Implant-Associated Orthopedic Infections. *Journal of Orthopaedic Research*: *Official Publication of the Orthopaedic Research Society*, **36**, 22-32. https://doi.org/10.1002/jor.23656

[3] Dias, C., Borges, A., Oliveira, D., Martinez-Murcia, A., Saavedra, M.J. and Simões, M. (2018) Biofilms and Antibiotic Susceptibility of Multidrug-Resistant Bacteria from Wild Animals. *PeerJ*, **6**, e4974. https://doi.org/10.7717/peerj.4974

[4] Baptista, P.V., McCusker, M.P., Carvalho, A., Ferreira, D.A., Mohan, N.M., Martins, M. and Fernandes, A.R. (2018) Nano-Strategies to Fight Multidrug Resistant Bacteria—A Battle of the Titans. *Frontiers in Microbiology*, **9**, 1441. https://doi.org/10.3389/fmicb.2018.01441

[5] Rigo, S., Cai, C., Gunkel-Grabole, G., Maurizi, L., Zhang, X., Xu, J. and Palivan, C.G. (2018) Nanoscience-Based Strategies to Engineer Antimicrobial Surfaces. *Advanced Science*, **5**, Article ID: 1700892. https://doi.org/10.1002/advs.201700892

[6] Baranwal, A., Srivastava, A., Kumar, P., Bajpai, V.K., Maurya, P.K. and Chandra, P. (2018) Prospects of Nanostructure Materials and Their Composites as Antimicrobial Agents. *Frontiers in Microbiology*, **9**, 422. https://doi.org/10.3389/fmicb.2018.00422

[7] Siddiqi, K.S., *et al*. (2018) Properties of Zinc Oxide Nanoparticles and Their Activity against Microbes. *Nanoscale Research Letters*, **13**, 141. https://doi.org/10.1186/s11671-018-2532-3

[8] Jiang, J., Pi, J. and Cai, J. (2018) The Advancing of Zinc Oxide Nanoparticles for Biomedical Applications. *Bioinorganic Chemistry and Applications*, **2018**, Article ID: 1062562. https://doi.org/10.1155/2018/1062562

[9] Tiwari, V., Mishra, N., Gadani, K., Solanki, P.S., Shah, N.A. and Tiwari, M. (2018) Mechanism of Anti-Bacterial Activity of Zinc Oxide Nanoparticle against Carbapenem-Resistant *Acinetobacter baumannii*. *Frontiers in Microbiology*, **9**, 1218. https://doi.org/10.3389/fmicb.2018.01218

[10] Pesci, F.M., Wang, G., Klug, D.R., Li, Y. and Cowan, A.J. (2013) Efficient Suppression of Electron-Hole Recombination in Oxygen-Deficient Hydrogen-Treated TiO(2) Nanowires for Photoelectrochemical Water Splitting. *The Journal of Physical Chemistry. C*, *Nanomaterials and Interfaces*, **117**, 25837-25844. https://doi.org/10.1021/jp4099914

[11] Gholap, H., Patil, R., Yadav, P., Banpurkar, A., Ogale, S. and Gade, W. (2013) CdTe-TiO_2 Nanocomposite: An Impeder of Bacterial Growth and Biofilm. *Nanotechnology*, **24**, Article ID: 195101. https://doi.org/10.1088/0957-4484/24/19/195101

[12] Chouhan, N., Yeh, C.L., Hu, S.-F., Liu, R.-S., Chang, W.-S. and Chen, K.-H. (2011) Photocatalytic CdSe QDs-Decorated ZnO Nanotubes: An Effective Photoelectrode for Splitting Water. *Chemical Communications*, **47**, 3493-3495. https://doi.org/10.1039/c0cc05548d

[13] Wang, G., Li, Z., Li, M., Chen, C., Lv, S. and Liao, J. (2016) Aqueous Phase Synthesis and Enhanced Field Emission Properties of ZnO-Sulfide Heterojunction Nanowires. *Scientific Reports*, **6**, Article No. 29470. https://doi.org/10.1038/srep29470

[14] An, L., Wang, G., Cheng, Y., Zhao, L., Gao, F. and Cheng, Y. (2015) Synthesis of CdS/ZnO Nanocomposite and Its Enhanced Photocatalytic Activity in Degradation

of Methyl Orange. *Russian Journal of Physical Chemistry A*, **89**, 1878-1883. https://doi.org/10.1134/S0036024415100180

[15] Jana, T.K., Maji, S.K., Pal, A., Maiti, R.P., Dolai, T.K. and Chatterjee, K. (2016) Photocatalytic and Antibacterial Activity of Cadmium Sulphide/Zinc Oxide Nanocomposite with Varied Morphology. *Journal of Colloid and Interface Science*, **480**, 9-16. https://doi.org/10.1016/j.jcis.2016.06.073

[16] Cao, S., Chen, Y., Kang, L., Lin, Z. and Fu, W.-F. (2015) Enhanced Photocatalytic H2-Evolution by Immobilizing CdS Nanocrystals on Ultrathin $Co_{0.85}Se$/RGO-PEI Nanosheets. *Journal of Materials Chemistry A*, **3**, 18711-18717. https://doi.org/10.1039/C5TA04910E

[17] Ozcan, C., Turkay, D. and Yerci, S. (2019) Optical and Electrical Design Guidelines for ZnO/CdS Nanorod-Based CdTe Solar Cells. *Optics Express*, **27**, A339-A351. https://doi.org/10.1364/OE.27.00A339

[18] Gholap, H., Warule, S., Sangshetti, J., Kulkarni, G., Banpurkar, A., Satpute, S. and Patil, R. (2016) Hierarchical Nanostructures of Au@ZnO: Antibacterial and Antibiofilm Agent. *Applied Microbiology and Biotechnology*, **100**, 5849-5858. https://doi.org/10.1007/s00253-016-7391-1

[19] Singh, S., Thiyagarajan, P., Mohan Kant, K., Anita, D., Thirupathiah, S., Rama, N., Tiwari, B., Kottaisamy, M. and Ramachandra Rao, M.S. (2007) Structure, Microstructure and Physical Properties of ZnO Based Materials in Various Forms: Bulk, Thin Film and Nano. *Journal of Physics D*: *Applied Physics*, **40**, 6312-6327. https://doi.org/10.1088/0022-3727/40/20/S15

[20] Liu, H., Zeng, F., Lin, Y., Wang, G. and Pan, F. (2013) Correlation of Oxygen Vacancy Variations to Band Gap Changes in Epitaxial ZnO Thin Films. *Applied Physics Letters*, **102**, Article ID: 181908. https://doi.org/10.1063/1.4804613

[21] Warule, S.S., Chaudhari, N.S., Shisode, R.T., Desa, K.V., Kale, B.B. and More, M.A. (2015) Decoration of CdS Nanoparticles on 3D Self-Assembled ZnO Nanorods: A Single-Step Process with Enhanced Field Emission Behaviour. *CrystEngComm*, **17**, 140-148. https://doi.org/10.1039/C4CE01738B

[22] Lipovsky, A., Gedanken, A. and Lubart, R. (2013) Visible Light-Induced Antibacterial Activity of Metaloxide Nanoparticles. *Photomedicine and Laser Surgery*, **31**, 526-530. https://doi.org/10.1089/pho.2012.3339

[23] Fu, P.P., Xia, Q., Hwang, H.-M., Ray, P.C. and Yu, H. (2014) Mechanisms of Nanotoxicity: Generation of Reactive Oxygen Species. *Journal of Food and Drug Analysis*, **22**, 64-75. https://doi.org/10.1016/j.jfda.2014.01.005

[24] Fan, W., Sun, Q., Li, Y., Tay, F.R. and Fan, B. (2018) Synergistic Mechanism of Ag(+)-Zn(2+) in Anti-Bacterial Activity against *Enterococcus faecalis* and Its Application against Dentin Infection. *Journal of Nanobiotechnology*, **16**, 10. https://doi.org/10.1186/s12951-018-0336-3

[25] Xie, Y., He, Y., Irwin, P.L., Jin, T. and Shi, X. (2011) Antibacterial Activity and Mechanism of Action of Zinc Oxide Nanoparticles against *Campylobacter jejuni*. *Applied and Environmental Microbiology*, **77**, 2325-2331. https://doi.org/10.1128/AEM.02149-10

[26] He, W., Kim, H.K., Wamer, W.G., Melka, D., Callahan, J.H. and Yin, J.J. (2014) Photogenerated Charge Carriers and Reactive Oxygen Species in ZnO/Au Hybrid Nanostructures with Enhanced Photocatalytic and Antibacterial Activity. *Journal of the American Chemical Society*, **136**, 750-757. https://doi.org/10.1021/ja410800y

[27] Sirelkhatim, A., Mahmud, S., Seeni, A., Kaus, N.H.M., Ann, L.C., Bakhori, S.K.M., Hasan, H. and Mohamad, D.J.N.-M.L. (2015) Review on Zinc Oxide Nanoparticles:

Antibacterial Activity and Toxicity Mechanism. *Nano-Micro Letters*, **7**, 219-242. https://doi.org/10.1007/s40820-015-0040-x

[28] Ramasamy, M., Das, M., An, S.S. and Yi, D.K. (2014) Role of Surface Modification in Zinc Oxide Nanoparticles and Its Toxicity Assessment toward Human Dermal Fibroblast Cells. *International Journal of Nanomedicine*, **9**, 3707-3718. https://doi.org/10.2147/IJN.S65086

[29] Wu, H., Moser, C., Wang, H.-Z., Høiby, N. and Song, Z.-J. (2014) Strategies for Combating Bacterial Biofilm Infections. *International Journal of Oral Science*, **7**, 1-7. https://doi.org/10.1038/ijos.2014.65

[30] Roy, R., Tiwari, M., Donelli, G. and Tiwari, V. (2018) Strategies for Combating Bacterial Biofilms: A Focus on Anti-Biofilm Agents and Their Mechanisms of Action. *Virulence*, **9**, 522-554. https://doi.org/10.1080/21505594.2017.1313372

[31] Singh, B.R., Singh, B.N., Singh, A., Khan, W., Naqvi, A.H. and Singh, H.B. (2015) Mycofabricated Biosilver Nanoparticles Interrupt *Pseudomonas aeruginosa* Quorum Sensing Systems. *Scientific Reports*, **5**, Article No. 13719. https://doi.org/10.1038/srep13719

[32] Ali, S.G., Ansari, M.A., Sajid Jamal, Q.M., Khan, H.M., Jalal, M., Ahmad, H. and Mahdi, A.A. (2017) Antiquorum Sensing Activity of Silver Nanoparticles in *P. aeruginosa*: An *in Silico* Study. *In Silico Pharmacology*, **5**, 12. https://doi.org/10.1007/s40203-017-0031-3